HHS Public Access

Author manuscript

Ophthalmology. Author manuscript; available in PMC 2024 September 15.

Published in final edited form as:

Ophthalmology. 2018 February ; 125(2): 255–266. doi:10.1016/j.ophtha.2017.08.030.

Natural History of Subclinical Neovascularization in Nonexudative Age-Related Macular Degeneration Using Swept-Source OCT Angiography

João R. de Oliveira Dias, MD, PhD[1], **Qinqin Zhang, PhD**[2], **José M.B. Garcia, MD**[1], **Fang Zheng, MD**[1,3], **Elie H. Motulsky, MD, PhD**[1], **Luiz Roisman, MD, PhD**[1], **Andrew Miller, MD**[1], **Chieh-Li Chen, PhD**[2], **Sophie Kubach, MS**[4], **Luis de Sisternes, PhD**[4], **Mary K. Durbin, PhD**[4], **William Feuer, MS**[1], **Ruikang K. Wang, PhD**[2], **Giovanni Gregori, PhD**[1], **Philip J. Rosenfeld, MD, PhD**[1]

[1]Department of Ophthalmology, Bascom Palmer Eye Institute, University of Miami Miller School of Medicine, Miami, Florida.

[2]Department of Bioengineering, University of Washington, Seattle, Washington.

[3]Department of Ophthalmology, Tianjin Medical University General Hospital, Tianjin Medical University, Tianjin, China.

[4]Research and Development (R&D), Carl Zeiss Meditec, Inc, Dublin, California.

Abstract

Purpose: Swept-source (SS) OCT angiography (OCTA) was used to determine the prevalence, incidence, and natural history of subclinical macular neovascularization (MNV) in eyes with nonexudative age-related macular degeneration (AMD).

Design: Prospective, observational, consecutive case series.

Participants: Patients with intermediate AMD (iAMD) or geographic atrophy (GA) secondary to nonexudative AMD in 1 eye and exudative AMD in the fellow eye.

Methods: All patients were imaged using both the 3×3 mm and 6×6 mm SS OCTA fields of view (PLEX Elite 9000; Carl Zeiss Meditec, Inc, Dublin, CA). The en face slab used to detect the MNV

Correspondence: Philip J. Rosenfeld, MD, PhD, Department of Ophthalmology, Bascom Palmer Eye Institute, University of Miami Miller School of Medicine, 900 NW 17th Street, Miami, FL 33136. prosenfeld@miami.edu.

Author Contributions:
Conception and design: de Oliveira Dias, Roisman, Wang, Gregori, Rosenfeld
Analysis and interpretation: de Oliveira Dias, Zhang, Garcia, Zheng, Motulsky, Roisman, Miller, Chen, Kubach, de Sisternes, Durbin, Feuer, Wang, Gregori, Rosenfeld
Data collection: de Oliveira Dias, Zhang, Garcia, Zheng, Motulsky, Roisman, Miller, Chen
Obtained funding: none
Overall responsibility: de Oliveira Dias, Zhang, Garcia, Zheng, Motulsky, Roisman, Miller, Chen, Kubach, de Sisternes, Durbin, Feuer, Wang, Gregori, Rosenfeld

Presented at: Angiogenesis, Exudation, and Degeneration Annual Meeting, Miami, Florida, February 2017; and as a poster at the Association for Research in Vision and Ophthalmology Annual Meeting, Baltimore, Maryland, May 2017.

HUMAN SUBJECTS: Human subjects were included in this study. The institutional review board of the University of Miami Miller School of Medicine approved the study, and informed consent to participate in the prospective OCT study was obtained from all patients. The study was performed in accordance with the tenets of the Declaration of Helsinki and complied with the Health Insurance Portability and Accountability Act of 1996.

extended from the outer retina to the choriocapillaris, and projection artifacts were removed using a proprietary algorithm.

Main Outcome Measures: Prevalence of subclinical MNV and time to exudation with Kaplan-Meier cumulative estimates of exudation at 1 year.

Results: From August 2014 through March 2017, 160 patients underwent SS OCTA (110 eyes with iAMD and 50 eyes with GA). Swept-source OCTA identified subclinical MNV at the time of first imaging in 23 of 160 eyes, for a prevalence of 14.4%. Six eyes demonstrated subclinical MNV during the follow-up. Of 134 eyes with follow-up visits, a total of 13 eyes demonstrated exudation, and of these 13 eyes, 10 eyes were found to have pre-existing subclinical MNV. By 12 months, the Kaplan-Meier cumulative incidence of exudation for all 134 eyes was 6.8%. For eyes with subclinical MNV at the time of first SS OCTA imaging, the incidence was 21.1%, and for eyes without subclinical MNV, the incidence was 3.6%. There was no difference in the cumulative incidence of exudation from pre-existing MNV in eyes with iAMD or GA ($P = 0.847$, log-rank test). After the detection of subclinical MNV, the risk of exudation was 15.2 times (95% confidence interval, 4.2–55.4) greater compared with eyes without subclinical MNV.

Conclusions: By 12 months, the risk of exudation was greater for eyes with documented subclinical MNV compared with eyes without detectable MNV. For eyes with subclinical MNV, recommendations include more frequent follow-up and home monitoring. Intravitreal therapy is not recommended until prospective studies are performed.

The onset of macular neovascularization (MNV) in age-related macular degeneration (AMD) typically has been defined by the onset of exudation. Historically, this macular exudation was diagnosed by fundus examination, by leakage during fluorescein angiography,[1] or by the appearance of macular fluid on OCT images.[2] Although indocyanine green angiography (ICGA) has proven useful for diagnosing type 1 MNV, which is a form of neovascularization that resides under the retinal pigment epithelium (RPE) and above Bruch's membrane,[3] ICGA is not useful for defining exudation. However, ICGA has been used to identify MNV even in the absence of exudation.[4–6] Although Sarks[7] and Green and Key[8] in the 1970s showed that MNV could exist in eyes with nonexudative AMD by performing histopathologic analyses of postmortem eyes, it was not until the mid 1990s that Schneider et al[4] and Hanutsaha et al[5] used ICGA to detect this subclinical neovascularization in situ in patients with nonexudative AMD. In these reports, patients with neovascular AMD in 1 eye and nonexudative AMD in the fellow eye underwent ICGA imaging, and in the eyes with nonexudative AMD, abnormal ICGA findings such as focal spots or ICGA plaques were identified and associated with an increased risk of exudation during the follow-up period. Although ICGA imaging could identify these subclinical lesions in situ before exudation occurred,[4–6] the significance and the potential usefulness of these findings for identifying patients at risk for exudation largely were ignored over the years, most likely because of the cost, risk, inconvenience, and discomfort associated with the use of ICGA as a screening tool in nonexudative AMD and because a viable therapeutic option was not available until the development of intravitreal inhibitors of vascular endothelial growth factor (VEGF) for the treatment of neovascular AMD.[9]

The recent development of swept-source (SS) OCT angiography (OCTA)[10–18] has greatly facilitated the detection of subclinical MNV and mitigated the limitations of ICGA. In contrast to ICGA, SS OCTA is a fast, noninvasive, safe, cost-effective, and easily performed imaging method that provides depth-resolved information about the MNV. The technique of SS OCTA imaging uses near-infrared light to acquire rapidly repeated B-scans (2-dimensional images acquired in the horizontal–axial plane of the retina) in the same position on the macula forming clusters, so that a decorrelation algorithm can be used to detect blood flow in the form of signal variation within a cluster.[13] These clusters can be acquired at multiple closely spaced locations in the vertical direction to form a cube of flow images characterizing the flow within the retina in 3 dimensions. These flow images then can be viewed as individual B-scans or as an en face image (in the horizontal–vertical plane) to reveal the retinal and choroidal microvasculature, including the MNV. This imaging strategy is ideal for identifying type 1 subclinical MNV in eyes with nonexudative AMD.[19–23]

Using SS OCTA, Roisman et al[22] were able to correlate subclinical MNV with the plaques seen on ICGA imaging in eyes with nonexudative AMD. In this study, 11 patients with exudative AMD in 1 eye and nonexudative AMD in the fellow eye were imaged with both ICGA and SS OCTA, and 3 eyes with nonexudative AMD were found to have both a plaque detected by ICGA and subclinical MNV detected by SS OCTA. In those eyes without evidence of ICGA abnormalities, SS OCTA did not identify any signs of MNV. Based on these encouraging results, additional patients with nonexudative AMD in 1 eye and exudative AMD in their fellow eye were enrolled and followed up to determine a more reliable estimate of the prevalence of MNV in these eyes with nonexudative AMD, the incidence of subclinical MNV over time, and the natural history of these subclinical lesions to determine their cumulative risk of exudation. In this report, we describe the natural history of these additional fellow eyes with nonexudative AMD and the time to exudation for eyes with and without previously identified subclinical MNV.

Methods

Patients with exudative AMD in 1 eye and nonexudative AMD in the fellow eye were enrolled from August 2014 through December 2016 and were followed up through March 2017 in a prospective, observational, consecutive OCT imaging study at the Bascom Palmer Eye Institute. The institutional review board of the University of Miami Miller School of Medicine approved the study, and informed consent to participate in the prospective OCT study was obtained from all patients. The study was performed in accordance with the tenets of the Declaration of Helsinki and complied with the Health Insurance Portability and Accountability Act of 1996.

Over the course of this study, from August 2014 through March 2017, patients underwent imaging with 3 different SS OCTA prototypes (recently made commercially available as PLEX Elite 9000; Carl Zeiss Meditec, Inc, Dublin, CA). The SS OCTA prototypes contained a SS laser with a central wavelength of approximately 1050 nm (1000–1100 nm full width) with a scanning rate of 100 000 A-scans per second. They had a full-width at half maximum axial resolution of approximately 5 μm in tissue and a lateral resolution at the retinal surface estimated at approximately 14 μm. For the 3×3 mm scans, the fast

scanning direction (i.e., transverse, *x*-axis) used 300 A-scans to form a single B-scan. Four consecutive B-scans were performed at each fixed location before proceeding to the next transverse location on the retina. In the slow-scanning direction (i.e., *y*-axis) there were 300 positions over a 3-mm distance. The spacing between adjacent B-scan positions was 10 μm. The time difference between 2 successive B-scans was roughly 4.2 ms, which corresponded to a B-scan acquisition rate of 238 B-scans per second.

The first SS OCTA prototype was able to perform only the 3×3 mm scans and did not have tracking. One limitation associated with this field of view was that the full extent of subclinical neovascular lesions that were larger than the scan area could not be visualized fully unless the scan was decentered away from the fovea. Another limitation was that a subclinical lesion outside the scan area could be missed. The second and third SS OCTA prototypes were able to perform 6×6 mm scans as well, and both had tracking. When the 6×6 mm scans were used, the full extent of the lesions could be identified, and no new diagnoses of subclinical neovascularization were found in these previously imaged eyes. The second SS OCTA prototype performed the 6×6 mm scans by using 420 A-scans per B-scan at 420 B-scan positions so that the spacing between adjacent A-scans and B-scans was 14.3 μm. The time difference between 2 successive B-scans was roughly 4.4 ms, which corresponded to a B-scan acquisition rate of 227 B-scans per second. The third SS OCTA prototype used 500 A-scans per B-scan at 500 B-scan positions for the 6×6 mm scans, resulting in an A-scan and B-scan separation of 12 μm. The time difference between 2 successive B-scans was roughly 5.2 ms, which corresponded to a B-scan acquisition rate of 192 B-scans per second. For all 3×3 mm scans, the B-scans were repeated 4 times at each B-scan position, and for all 6×6 mm scans, the B-scans were repeated twice at each position.

The motion-contrast algorithm used to process all the OCTA datasets to create flow images is known as optical microangiography.[17,24–27] This algorithm was used to create both B-scans and en face flow images.[28] The segmentation strategy used to create the slab for visualization of the MNV extended from the bottom boundary of the outer plexiform layer to 8 μm beneath Bruch's membrane, which included the inner portion of the choriocapillaris, as previously described.[22] This en face slab from the outer retina-to-choriocapillaris was designated as the ORCC slab. Projection artifacts were removed for better visualization of the MNV using a proprietary algorithm that has been described previously.[12,18]

In addition to SS OCTA imaging, all patients underwent spectral-domain (SD) OCT imaging (Cirrus AngioPlex; Carl Zeiss Meditec, Inc) by the same technician during the same imaging session. Spectral-domain OCT imaging included the 6×6 mm structural images that comprised 200 A-scans per B-scan at 200 B-scan positions.

Eyes with nonexudative AMD were classified by retina specialists (J.R.d.O.D., P.J.R.) based on fundus examination and SD OCT imaging results as either intermediate AMD (iAMD) or late AMD using the classification scheme described previously.[29] Intermediate AMD was defined by the presence of drusen and pigmentary abnormalities in the central macula without evidence of geographic atrophy (GA) or exudation. Late nonexudative AMD was defined by the presence of GA in the absence of exudation. The presence of subclinical MNV was diagnosed after the review of both SS OCT B-scans with color-coded

flow and outer retina-to-choriocapillaris images with and without flow in the absence of exudative signs and confirmed by at least 2 retina specialists (J.R.d.O.D., P.J.R.). To identify subclinical MNV, the retina specialists inspected the en face outer retina-to-choriocapillaris (ORCC) slab flow image after removal of retinal vessel projection artifacts. Then, before any flow signal on the en face image could be confirmed as subclinical MNV, the flow signal had to be validated by examining representative B-scans with superimposed color-coded flow to localize the neovascular lesion to the appropriate layer.

Cumulative rates of incidence of exudation were calculated with the Kaplan-Meier method and compared between groups with the log-rank test. Because subclinical MNV was not always present when the first SS image was obtained, the ratio of risk of exudation with and without subclinical MNV was estimated with a Cox proportional hazards survival analysis in which observation of subclinical MNV was included as a time-dependent covariate. Time to symptomatic exudation was defined as the day the patient received treatment with intravitreal anti-VEGF therapy.

Results

One hundred sixty consecutive patients with exudative AMD in one eye and nonexudative AMD in the fellow eye were enrolled between August 2014 and December 2016, with their last follow-up with SS OCTA imaging through March 2017. Of 160 eyes with nonexudative AMD, 110 eyes were diagnosed with iAMD (61.8% women) and 50 eyes were diagnosed with late AMD (60% women). Overall, ages ranged from 50 to 96 years, with a mean age of 79.6 years. The mean age of the iAMD group was 78.6 years and that of the late AMD group was 81.9 years.

Prevalence and Natural History

Overall, SS OCTA identified subclinical MNV at the time of the first imaging session in 23 of 160 eyes, for a prevalence of 14.4%. In the eyes with nonexudative AMD, subclinical MNV was found in 15 eyes with iAMD (13.6%) and in 8 eyes with late AMD (16.0%; $P = 0.808$, Fisher exact test). All of the 23 eyes in which a subclinical MNV was identified at first imaging contained type 1 MNV.

A total of 134 eyes were followed up. Of these 134 eyes, 90 were diagnosed with iAMD and 44 were diagnosed with late nonexudative AMD at baseline. For these 134 eyes, follow-up ranged from 1 to 31 months, with a mean follow-up of 16 months. Figures 1 to 4 represent 2 eyes with iAMD that were diagnosed with subclinical MNV at baseline and followed up over 18 months and 17 months, respectively, using both 3×3 mm scans (Figs 1 and 3) and 6×6 mm scans (Figs 2 and 4). These eyes did not demonstrate any evidence of exudation during the follow-up period. Of the 134 eyes that were followed up, 13 eyes demonstrated exudation (6.8% cumulative 1-year Kaplan-Meier incidence of exudation). Figures 5 to 7 depict eyes with subclinical MNV at baseline that demonstrated exudation during the follow-up period. The eye shown in Figure 5 demonstrated symptomatic exudation 24 months after the subclinical type 1 MNV was diagnosed at baseline. The eye shown in Figure 6 demonstrated exudation that was associated with type 3 MNV that developed during the follow-up period. This eye eventually was treated when the lesion became

symptomatic at 11 months of follow-up. Figure 7 depicts an eye that demonstrated multiple foci of subclinical MNV in which just one of the neovascular lesions was found to grow and eventually demonstrate exudation. This eye was treated after 18 months of follow-up. Figure 8 depicts an eye that demonstrated exudation associated with subretinal hyperreflective material. This neovascular lesion was not detected before exudation, but appeared to arise at the site of a pre-existing druse as seen on the B-scan. Twenty-two of 23 eyes with subclinical MNV at initial SS OCTA had more than 1 visit. Using the Kaplan-Meier method to estimate the cumulative incidence of exudation by 1 year of follow-up, we found a statistically significant difference ($P < 0.001$, log-rank test) between eyes with subclinical MNV at initial SS OCTA imaging (n = 22), of which 21.1% cumulatively demonstrated exudation within 1 year of follow-up, and eyes without subclinical MNV (n = 112), of which 3.6% cumulatively demonstrated exudation within 1 year (Fig 9).

Among the 112 eyes without subclinical MNV at initial SS OCT imaging, 6 eyes demonstrated subclinical MNV during the follow-up at periods ranging from 4 to 18 months. The cumulative incidence of subclinical MNV was 5.4% at 1 year of follow-up. When calculating the incidence of exudation from the time of first observation of any subclinical MNV, either at baseline or during follow-up, the incidence was 24% at 1 year of follow-up (Fig 10). In an analysis using all 134 eyes with more than 1 visit, the risk of exudation developing at 1 year rose dramatically by a factor of 15.2 (95% confidence interval, 4.2–55.4) after the observation of subclinical MNV ($P < 0.001$, time-dependent Cox proportional hazards regression) compared with eyes without subclinical MNV. Among eyes with subclinical MNV, there was no difference in the incidence of exudation between those with intermediate AMD and those with GA ($P = 0.847$, log-rank test). In an analysis using all 134 eyes with more than 1 visit, the risk of exudation developing was not associated with the type of nonexudative AMD ($P = 0.625$, time-dependent Cox proportional hazards regression). Of the 6 eyes in which a subclinical MNV was identified during follow-up intervals, 5 eyes demonstrated type 1 MNV and 1 eye was found to have early subclinical type 3 MNV (Fig 6).

Of the 3 eyes that demonstrated exudation without prior diagnosis of subclinical MNV, all the eyes were diagnosed with iAMD and were found to have pre-existing small elevations of the RPE at the site where the MNV eventually developed. One eye that demonstrated exudation had not been imaged with SS OCTA for 19 weeks before the onset of exudation. This was the result of technical issues in which the prototype SS OCTA instrument was not operational when the patient was seen 13 weeks before the onset of exudation. However, this patient did undergo SD OCTA imaging, and a new elevation of the RPE was diagnosed at the site where exudative MNV eventually developed. The other 2 eyes that demonstrated exudation without prior diagnosis of subclinical MNV also showed prior druse-like elevations of the RPE at the site of eventual exudation, but 1 eye had not been imaged with SS OCTA for 8 weeks before the onset of exudation (Fig 8), and the other eye had not been imaged with SS OCTA for 44 weeks before onset. For this eye that did not have a prior diagnosis of subclinical MNV and had a 44-week delay in imaging, the delay was the result of medical complications that developed after the patient traveled north for the summer months.

Discussion

Swept-source OCTA imaging identified subclinical MNV in 14.4% of 160 eyes with nonexudative AMD in which the fellow eye already had demonstrated exudative AMD. There was no difference in the prevalence of subclinical MNV in eyes with iAMD or late nonexudative AMD with GA. Of the 112 eyes without subclinical MNV at baseline, the cumulative incidence of subclinical MNV was 5.4% at 1 year of follow-up. Remarkably, if subclinical MNV was detected, the risk of exudation developing rose dramatically by a factor of 15.2 (95% confidence interval, 4.2–55.4) compared with eyes without subclinical MNV.

In all the eyes that demonstrated exudation without the prior detection of subclinical MNV, a druse-like elevation could be identified at the site of exudation where the MNV developed. We believe that these RPE elevations were the first sign of type 1 MNV and can serve as harbingers of impending exudation, and if more frequent SS OCTA imaging had been performed in these patients, a subclinical lesion might have been identified.

Although the vast majority of the neovascular lesions were classified as type 1 MNV, there was 1 case of type 3 MNV (Fig 6). Not surprisingly, for all the type 1 neovascular lesions, there was some elevation of the RPE associated with the MNV even before exudation developed. Even in the 3 patients in which a subclinical lesion was not identified, the RPE elevation was present. In 1 of the 3 patients, the exudation developed within 8 weeks of prior imaging and was associated with subretinal hyperreflective material. In the remaining 2 cases where a subclinical MNV was not detected, 1 patient was not imaged for 44 weeks because of an absence from South Florida and the other patient was not imaged for 19 weeks because of the lack of an operational SS OCTA instrument at the time of routine follow-up.

The 6.8% 1-year rate of exudation that we identified in eyes of patients with nonexudative AMD in which the fellow eye had exudative AMD was similar to the rates found in the Comparison of Age-Related Macular Degeneration Treatment Trials (CATT).[30] In CATT, the overall incidence of MNV and exudation in the fellow eye after 1 year was 7.9% in patients treated with ranibizumab and 7.2% in patients treated with bevacizumab; after 2 years these rates were 20.6% and 16.6%, respectively. However, in the Minimally Classic/Occult Trial of the Anti-VEGF Antibody Ranibizumab in the Treatment of Neovascular Age-Related Macular Degeneration (MARINA), the conversion rates at 1 year for the 0.3-mg and 0.5-mg ranibizumab groups were 20% and 21%, respectively, and that in the sham group was 26%.[31] In the Anti-VEGF Antibody for the Treatment of Predominantly Classic Choroidal Neovascularization in Age-Related Macular Degeneration (ANCHOR) study, 15.9% of fellow eyes converted in the 0.3-mg ranibizumab group by 12 months and 23.8% of such eyes converted by 24 months. The conversion rate in the 0.5-mg ranibizumab group was 24.3% and 35.1% by 12 and 24 months, respectively.[31] Although it is not immediately obvious why our rates are similar to those of CATT and lower than ranibizumab studies, possible explanations are that CATT enrolled patients more recently than the MARINA and ANCHOR trials and that OCT imaging was not performed routinely in the MARINA and ANCHOR trials. Consequently, when MARINA and ANCHOR patients were enrolled, the eyes with exudative disease were probably more advanced than in CATT, so the likelihood

of the fellow eye having subclinical lesions would have been greater, and early exudative changes in the fellow eyes may have been missed in the MARINA and ANCHOR studies by the absence of OCT imaging, thus setting the stage for a higher occurrence of exudation in the fellow eyes as the studies progressed.

Our study suggested that SS OCTA should be able to identify the vast majority of eyes with nonexudative AMD in which exudation will develop. Although we studied only eyes with nonexudative AMD in which the fellow eye already had exudative disease, we predict that SS OCTA imaging should be just as useful for detecting these subclinical neovascular lesions even when both eyes are diagnosed with nonexudative AMD. Moreover, based on recent studies reporting on the superiority of detecting known MNV with SS OCTA compared with SD OCTA, it would be reasonable to conclude that SS OCTA would be superior to SD OCTA in detecting subclinical MNV as well.[14,16] The superiority of SS OCTA for the detection of type 1 MNV is likely because of the reduced sensitivity roll-off from the SS OCT technology and the longer wavelength of the SS OCT instrument resulting in reduced scattering and absorption by the RPE complex and deeper penetration of light into the choroid with better detection of MNV under the RPE.[14,16]

For eyes with subclinical MNV, the current recommendation is to monitor these eyes more closely. This can be achieved by encouraging vigilant home monitoring with frequent vision testing combined with more frequent clinic visits. This home monitoring can involve testing of reading vision from each eye, using the Amsler grid or using the more advanced vision-monitoring technologies. The goal of this monitoring is to detect the earliest signs of exudation that affect a patient's visual function. Because some eyes can persist with subclinical MNV for 1 year or longer and can show neovascular lesion growth with good vision, these lesions may be beneficial and may provide nutritional support to the overlying RPE and photoreceptors. For this reason, we do not recommend treatment with anti-VEGF therapy, even if the subclinical lesion is growing. After all, if the goal of anti-VEGF therapy is to maintain a fluid-free macula and there was never any fluid in the macula, then in such a scenario, if anti-VEGF therapy were to be started, when would the treatment ever be stopped? If the answer is that the treatment would be stopped when the subclinical MNV is no longer detected, then treatment likely would continue until GA develops because experience tells us that type 1 MNV can no longer be detected only after atrophy arises. Then, there would be lingering question as to whether the treatment had been detrimental by accelerating the formation of GA. Because of this concern, anti-VEGF therapy should not be performed on eyes with subclinical lesions until a randomized clinical trial is performed to determine if the treatment is beneficial or detrimental over a prolonged period.

Detection of subclinical MNV also is very important when recruiting nonexudative AMD patients into clinical trials for the study of experimental therapies. It would be important to identify and stratify patients at baseline using SS OCTA to determine whether subclinical MNV is present, because these eyes would be more likely to demonstrate exudation during the course of the trial. An imbalance at baseline of these lesions may lead to erroneous conclusions as to whether the experimental treatment promotes or suppresses exudation. Moreover, it is also important to understand the effect of any new treatment on pre-existing MNV. Therefore, for these reasons, it is imperative that SS OCTA imaging be included in all

future trials that study eyes with nonexudative AMD eyes. In addition, a new terminology is needed to describe this subclinical, neovascular stage of AMD. One possible strategy would be to subdivide nonexudative AMD into nonneovascular and neovascular stages, with the actual development of exudation signaling the progression to late exudative AMD.

The main limitation of this study is that we did not have a defined follow-up schedule for all patients because the follow-up was determined by the need for anti-VEGF therapy in the fellow eye with known exudative disease. These variable follow-up intervals may have contributed to our inability to detect subclinical MNV in just 1 of the 3 patients who demonstrated exudation without prior detection of subclinical neovascularization, and this patient was lost to follow-up because of a prolonged illness. Because of the variable follow-up intervals, we elected to report the time to treatment as the incidence rate rather than the time to exudation because some patients sought treatment when they were symptomatic and some patients were followed up with minimal exudation until they became symptomatic and required treatment. Another limitation of this study was the lack of at least 2 years of follow-up for all eyes. However, a prospective study with scheduled follow-up intervals over 2 years is about to be initiated by the Advanced Retinal Imaging Network using SS OCTA. Although it would have been useful to compare SD OCTA imaging on all eyes to determine if a commercially available SD OCTA instrument would have been able to detect all the subclinical MNV observed using the SS OCTA instrument, we do know from previous studies that SD OCTA imaging is unable to detect the full extent of the MNV compared with SS OCTA imaging, so it is reasonable to assume that SD OCTA may not have detected the smaller subclinical lesions.[14,16]

With the growing availability of SS OCTA and the ability to acquire both structure and flow information noninvasively from a single SS OCT dataset, it is reasonable to suggest that OCT imaging will replace most, if not all, of the current imaging now performed using dye-based angiography for the routine management of AMD patients. We expect that the early detection of subclinical MNV before exudation develops should help us to educate patients about the disease, and with this increased appreciation of potential vision loss combined with improved home monitoring and more frequent clinic visits, we should be able to treat earlier with anti-VEGF therapy, resulting in better visual acuity outcomes. In addition, for clinical trials investigating novel therapies for the treatment of nonexudative AMD, it is imperative to include SS OCTA imaging to identify those eyes with subclinical MNV at baseline and as the study progresses. Because development of exudation would be an important end point in any nonexudative AMD study, some studies will elect to exclude these patients from enrollment, whereas other studies will want to follow up these patients and determine if the experimental therapy has any effect on the appearance, growth, and progression of these subclinical lesions.

In summary, we report on the prevalence, incidence, and natural history of subclinical MNV in eyes with nonexudative AMD imaged with SS OCTA. The vast majority of those eyes that demonstrate exudation after 1 year were found to have subclinical MNV, with a 15-fold higher risk of exudation developing compared with eyes without detectable MNV. By using a dependable, fast, cost-effective, and safe method for the easy detection of subclinical

MNV, we can identify eyes at risk for exudation and predict more reliably the future clinical course for these eyes.

Financial Disclosure(s):

The author(s) have made the following disclosure(s): J.R.d.O.D.: Financial support - Carl Zeiss Meditec, Inc.

Q.Z.: Financial support - Carl Zeiss Meditec, Inc.

E.H.M.: Financial support - Carl Zeiss Meditec, Inc.

S.K.: Employee - Carl Zeiss Meditec, Inc.

L.d.S.: Employee - Carl Zeiss Meditec, Inc.

M.K.D.: Employee - Carl Zeiss Meditec, Inc.

R.K.W.: Financial support and Patent - Carl Zeiss Meditec, Inc; Equity owner - Carl Zeiss Meditec, Inc, Kowa, Inc.

G.G.: Financial support and Patent - Carl Zeiss Meditec, Inc.

P.J.R.: Consultant - Carl Zeiss Meditec, Inc, Acucela, Boehringer-Ingelheim, Cell Cure Neurosciences, Chengdu Kanghong Biotech, Genentech, Healios K.K, F. Hoffmann-La Roche Ltd, Isarna Pharmaceuticals, MacRegen, Inc, Ocudyne, Ocunexus Therapeutics, Tyrogenex, Unity Biotechnology; Financial support - Carl Zeiss Meditec, Inc, Apellis, Genentech, Tyrogenex; Equity owner - Apellis, Digisight, Ocudyne

Supported by Carl Zeiss Meditec, Inc, Dublin, California; the National Eye Institute, National Institutes of Health, Bethesda, Maryland (grant nos.: R01EY024158 and P30EY014801 [Department of Ophthalmology, University of Miami Miller School of Medicine]); an unrestricted grant from the Research to Prevent Blindness, Inc, New York, New York (R.K.W.); and the CAPES Foundation, Ministry of Education of Brazil, Brasília, Brazil (L.R.). The funding organizations had no role in the design or conduct of this research.

Abbreviations and Acronyms:

AMD	age-related macular degeneration
ANCHOR	Anti-VEGF Antibody for the Treatment of Predominantly Classic Choroidal Neovascularization in Age-Related Macular Degeneration
CATT	Comparison of Age-Related Macular Degeneration Treatment Trials
GA	geographic atrophy
iAMD	intermediate age-related macular degeneration
ICGA	indocyanine green angiography
MARINA	Minimally Classic/Occult Trial of the Anti-VEGF Antibody Ranibizumab in the Treatment of Neovascular Age-Related Macular Degeneration
MNV	macular neovascularization
OCTA	OCT angiography
ORCC	outer retina-to-choriocapillaris
RPE	retinal pigment epithelium

SD	spectral-domain
SHRM	subretinal hyperreflective material
SS	swept-source
VEGF	vascular endothelial growth factor

References

1. Gess AJ, Fung AE, Rodriguez JG. Imaging in neovascular age-related macular degeneration. Semin Ophthalmol. 2011;26(3):225–233. [PubMed: 21609236]
2. Rosenfeld PJ. Optical coherence tomography and the development of antiangiogenic therapies in neovascular age-related macular degeneration. Invest Ophthalmol Vis Sci. 2016;57(9): OCT14–OCT26. [PubMed: 27409464]
3. Guyer DR, Yannuzzi LA, Slakter JS, et al. Classification of choroidal neovascularization by digital indocyanine green videoangiography. Ophthalmology. 1996;103(12):2054–2060. [PubMed: 9003339]
4. Schneider U, Gelisken F, Inhoffen W, Kreissig I. Indocyanine green angiographic findings in fellow eyes of patients with unilateral occult neovascular age-related macular degeneration. Int Ophthalmol. 1997;21(2):79–85. [PubMed: 9405989]
5. Hanutsaha P, Guyer DR, Yannuzzi LA, et al. Indocyanine-green videoangiography of drusen as a possible predictive indicator of exudative maculopathy. Ophthalmology. 1998;105(9):1632–1636. [PubMed: 9754169]
6. Querques G, Srour M, Massamba N, et al. Functional characterization and multimodal imaging of treatment-naive “quiescent” choroidal neovascularization. Invest Ophthalmol Vis Sci. 2013;54(10):6886–6892. [PubMed: 24084095]
7. Sarks SH. New vessel formation beneath the retinal pigment epithelium in senile eyes. Br J Ophthalmol. 1973;57(12): 951–965. [PubMed: 4788954]
8. Green WR, Key SN 3rd. Senile macular degeneration: a histopathologic study. Trans Am Ophthalmol Soc. 1977;75: 180–254. [PubMed: 613523]
9. Campochiaro PA, Aiello LP, Rosenfeld PJ. Anti-vascular endothelial growth factor agents in the treatment of retinal disease: from bench to bedside. Ophthalmology. 2016;123(10S):S78–S88. [PubMed: 27664289]
10. Moult E, Choi W, Waheed NK, et al. Ultrahigh-speed swept-source OCT angiography in exudative AMD. Ophthalmic Surg Lasers Imaging Retina. 2014;45(6):496–505. [PubMed: 25423628]
11. Zhang A, Wang RK. Feature space optical coherence tomography based micro-angiography. Biomed Opt Express. 2015;6(5):1919–1928. [PubMed: 26137391]
12. Zhang A, Zhang Q, Wang RK. Minimizing projection artifacts for accurate presentation of choroidal neovascularization in OCT micro-angiography. Biomed Opt Express. 2015;6(10): 4130–4143. [PubMed: 26504660]
13. Zhang A, Zhang Q, Chen CL, Wang RK. Methods and algorithms for optical coherence tomography-based angiography: a review and comparison. J Biomed Opt. 2015;20(10):100901. [PubMed: 26473588]
14. Novais EA, Adhi M, Moult EM, et al. Choroidal neovascularization analyzed on ultrahigh-speed swept-source optical coherence tomography angiography compared to spectral-domain optical coherence tomography angiography. Am J Ophthalmol. 2016;164:80–88. [PubMed: 26851725]
15. Lane M, Moult EM, Novais EA, et al. Visualizing the choriocapillaris under drusen: comparing 1050-nm swept-source versus 840-nm spectral-domain optical coherence tomography angiography. Invest Ophthalmol Vis Sci. 2016;57(9):OCT585–OCT590. [PubMed: 27547891]
16. Miller AR, Roisman L, Zhang Q, et al. Comparison between spectral-domain and swept-source optical coherence tomography angiographic imaging of choroidal neovascularization. Invest Ophthalmol Vis Sci. 2017;58(3):1499–1505. [PubMed: 28273316]

17. Zhang Q, Chen CL, Chu Z, et al. Automated quantitation of choroidal neovascularization: a comparison study between spectral-domain and swept-source OCT angiograms. Invest Ophthalmol Vis Sci. 2017;58(3):1506–1513. [PubMed: 28273317]
18. Zhang Q, Zhang A, Lee CS, et al. Projection artifact removal improves visualization and quantitation of macular neovascularization imaged by optical coherence tomography angiography. Ophthalmol Retina. 2017;1(2):124–136. [PubMed: 28584883]
19. Nehemy MB, Brocchi DN, Veloso CE. Optical coherence tomography angiography imaging of quiescent choroidal neovascularization in age-related macular degeneration. Ophthalmic Surg Lasers Imaging Retina. 2015;46(10):1056–1057. [PubMed: 26599251]
20. Palejwala NV, Jia Y, Gao SS, et al. Detection of nonexudative choroidal neovascularization in age-related macular degeneration with optical coherence tomography angiography. Retina. 2015;35(11):2204–2211. [PubMed: 26469533]
21. Querques G, Souied EH. Vascularized drusen: slowly progressive type 1 neovascularization mimicking drusenoid retinal pigment epithelium elevation. Retina. 2015;35(12):2433–2439. [PubMed: 26418449]
22. Roisman L, Zhang Q, Wang RK, et al. Optical coherence tomography angiography of asymptomatic neovascularization in intermediate age-related macular degeneration. Ophthalmology. 2016;123(6):1309–1319. [PubMed: 26876696]
23. Carnevali A, Cicinelli MV, Capuano V, et al. Optical coherence tomography angiography: a useful tool for diagnosis of treatment-naive quiescent choroidal neovascularization. Am J Ophthalmol. 2016;169:189–198. [PubMed: 27394033]
24. Wang RK, An L, Francis P, Wilson DJ. Depth-resolved imaging of capillary networks in retina and choroid using ultrahigh sensitive optical microangiography. Opt Lett. 2010;35(9):1467–1469. [PubMed: 20436605]
25. Reif R, Qin J, An L, et al. Quantifying optical microangiography images obtained from a spectral domain optical coherence tomography system. Int J Biomed Imaging. 2012;2012:509783. [PubMed: 22792084]
26. Huang Y, Zhang Q, Thorell MR, et al. Swept-source OCT angiography of the retinal vasculature using intensity differentiation-based optical microangiography algorithms. Ophthalmic Surg Lasers Imaging Retina. 2014;45(5):382–389. [PubMed: 25230403]
27. Wei W, Xu J, Baran U, et al. Intervolume analysis to achieve four-dimensional optical microangiography for observation of dynamic blood flow. J Biomed Opt. 2016;21(3):36005. [PubMed: 26968387]
28. Yin X, Chao JR, Wang RK. User-guided segmentation for volumetric retinal optical coherence tomography images. J Biomed Opt. 2014;19(8):086020. [PubMed: 25147962]
29. Ferris FL 3rd, Wilkinson CP, Bird A, et al. Clinical classification of age-related macular degeneration. Ophthalmology. 2013;120(4):844–851. [PubMed: 23332590]
30. Maguire MG, Daniel E, Shah AR, et al. Incidence of choroidal neovascularization in the fellow eye in the comparison of age-related macular degeneration treatments trials. Ophthalmology. 2013;120(10):2035–2041. [PubMed: 23706946]
31. Barbazetto I, Saroj N, Shapiro H, et al. Incidence of new choroidal neovascularization in fellow eyes of patients treated in the MARINA and ANCHOR trials. Am J Ophthalmol. 2010;149(6):939–946.e931. [PubMed: 20378094]

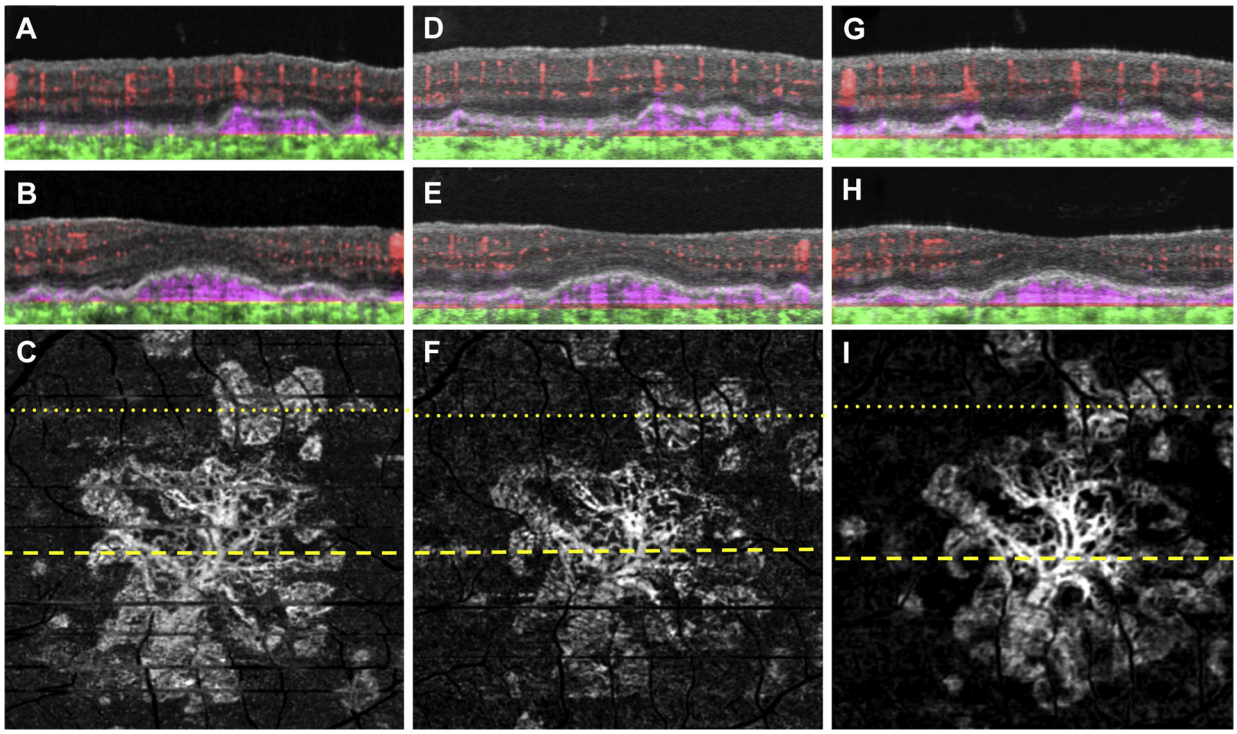

Figure 1.

Swept-source OCT angiography (OCTA; 3×3 mm) of an asymptomatic eye from a patient with nonexudative age-related macular degeneration followed up for 18 months without exudation. **A**, **B**, Optical coherence tomography B-scan (**A**) superior to the fovea and (**B**) through the fovea with colorcoded flow represented as *red* for the retinal microvasculature, *pink* for the outer retina-to-choriocapillaris (ORCC) slab, and *green* for the remainder of the choroid. Note the *pink* coloration under the retinal pigment epithelium and above Bruch's membrane, which represents the type 1 macular neovascularization. **C**, Swept-source OCTA en face ORCC slab image with removal of retinal vessel projection artifacts showing a multilobular and multifocal neovascular complex that extends to the boundaries of scan area. The dotted and dashed lines represent the B-scans contained in (**A**) and (**B**), respectively. **D**, **E**, Images obtained 4 months after those in (**A**–**C**): OCT B-scans with color-coded flow (**D**) superior to the fovea and (**E**) through the fovea. **F**, Swept-source OCTA en face ORCC slab image with removal of retinal vessel projection artifacts. The dotted and dashed lines represent the B-scans contained in (**D**) and (**E**), respectively. **G**, **H**, Images obtained 14 months after those in (**D**–**F**): OCT B-scans with color-coded flow (**G**) superior to the fovea and (**H**) through the fovea. **I**, Swept-source OCTA en face ORCC slab image with removal of retinal vessel projection artifacts. The dotted and dashed lines represent the B-scans contained in (**G**) and (**H**), respectively.

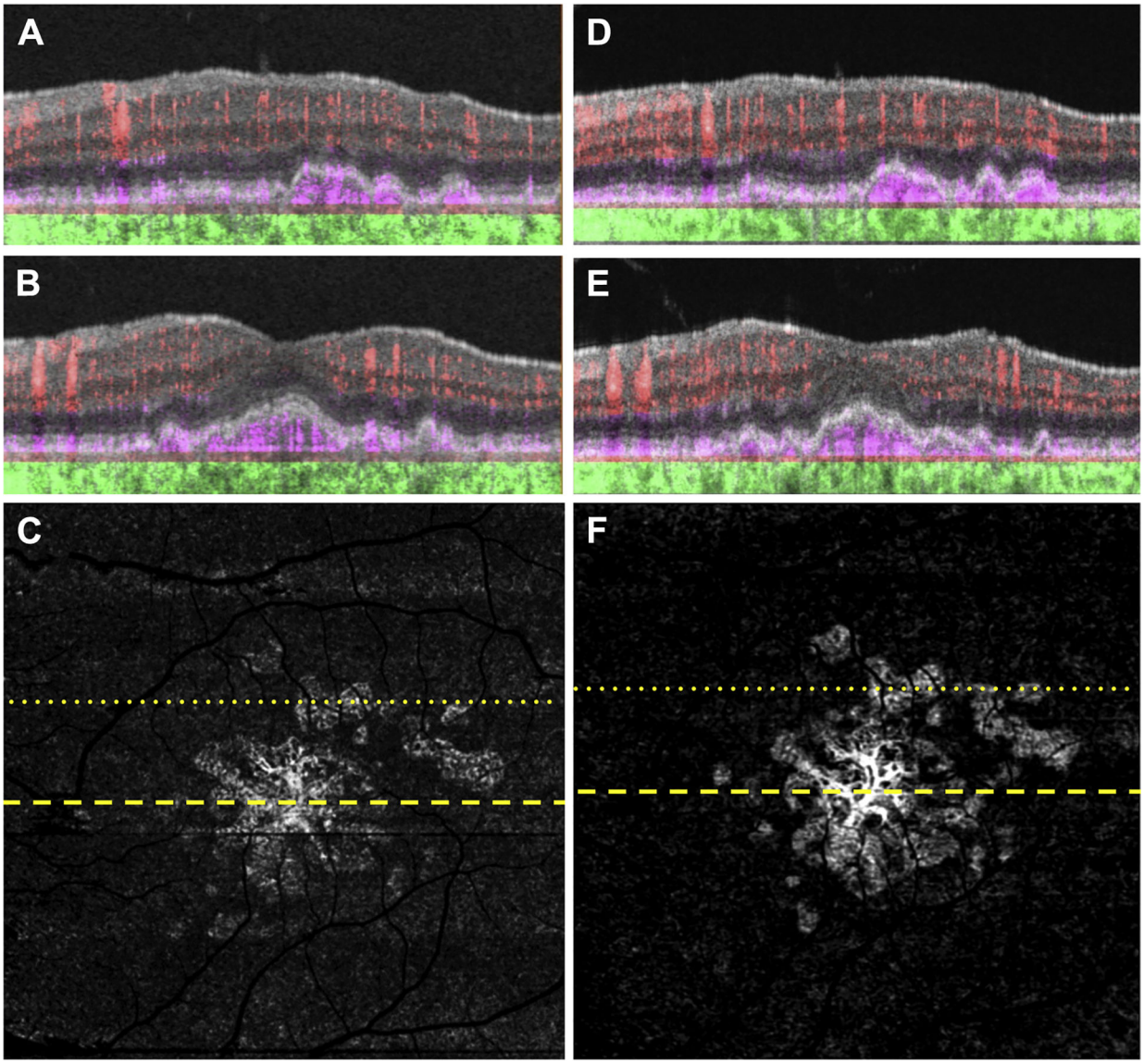

Figure 2.

Swept-source (SS) OCT angiography (OCTA) of the same eye as in Figure 1 imaged using a 6×6 mm scan. **A**, **B**, Optical coherence tomography B-scan (**A**) superior to the fovea and (**B**) through the fovea with color-coded flow represented as *red* for the retinal microvasculature, *pink* for the outer retina-to-choriocapillaris (ORCC) slab, and *green* for the remainder of the choroid. Note the *pink* coloration under the retinal pigment epithelium and above Bruch's membrane, which represents the type 1 macular neovascularization. **C**, Swept-source OCTA en face ORCC slab image with removal of retinal vessel projection artifacts showing macular neovascularization that is multilobular and multifocal with a total area of 4.70 mm^2 as determined by using an automated quantification algorithm that was described previously.[17] The dotted and dashed lines represent the B-scans contained in (**A**) and (**B**), respectively. The 6×6 mm scans could not be performed by the prototype SS OCTA instrument before this visit. **D**, **E**, Images obtained 14 months after those in (**A**–**C**): OCT B-scans with color-coded flow (**D**) superior to the fovea and (**E**) through the fovea. **F**,

Swept-source OCTA en face ORCC slab image with removal of retinal vessel projection artifacts showing a neovascular lesion with an area of 5.11 mm^2. The dotted and dashed lines represent the B-scans contained in (**D**) and (**E**), respectively.

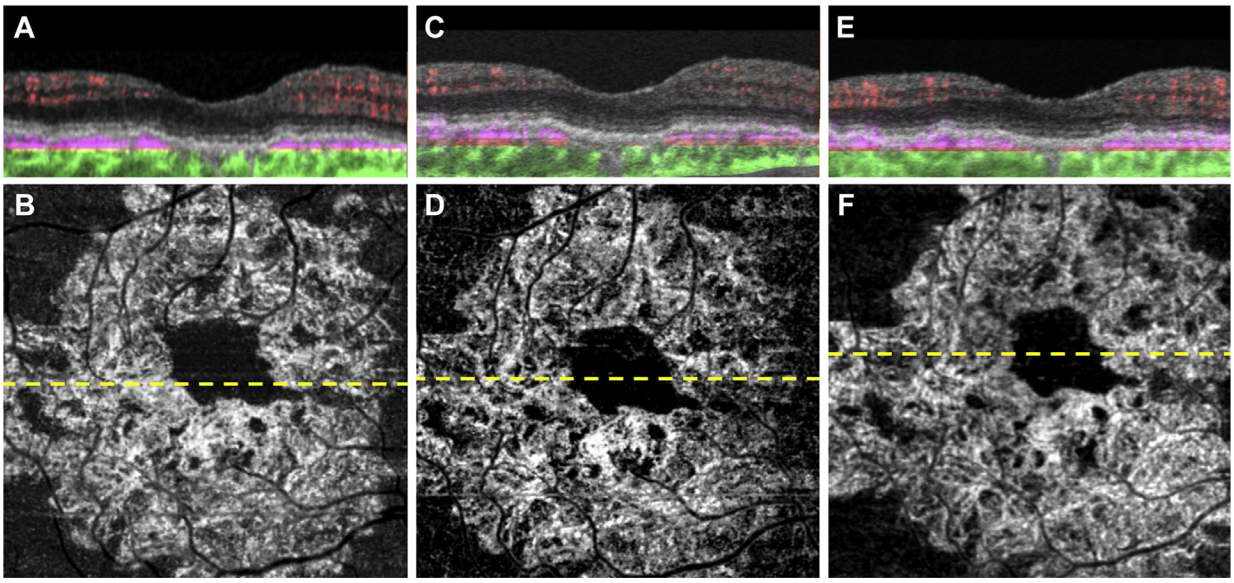

Figure 3.

Swept-source OCT angiography (OCTA; 3×3 mm) of an asymptomatic eye from a patient with nonexudative age-related macular degeneration followed up for 17 months without exudation. **A**, Optical coherence tomography B-scan through the fovea with color-coded flow represented as *red* for the retinal microvasculature, *pink* for the outer retina-to-choriocapillaris (ORCC) slab, and *green* for the remainder of the choroid. Note the *pink* coloration under the retinal pigment epithelium and above Bruch's membrane, which represents the type 1 macular neovascularization. **B**, Swept-source OCTA en face ORCC slab image with removal of retinal vessel projection artifacts showing a wreath-shaped neovascular complex that extends to the boundaries of scan area. The dashed line represents the B-scan contained in (**A**). **C**, **D**: Images obtained 3 months after those in (**A**, **B**). **C**, OCT B-scan with color-coded flow through the fovea. **D**, Swept-source OCTA en face ORCC slab image with removal of retinal vessel projection artifacts. The dashed line represents the B-scan contained in (**C**). **E**, **F**: Images obtained 14 months after those in (**C**, **D**). **E**, OCT B-scan with color-coded flow through the fovea. **F**, Swept-source OCTA en face ORCC slab image with removal of retinal vessel projection artifacts. The dashed line represents the B-scan contained in (**E**).

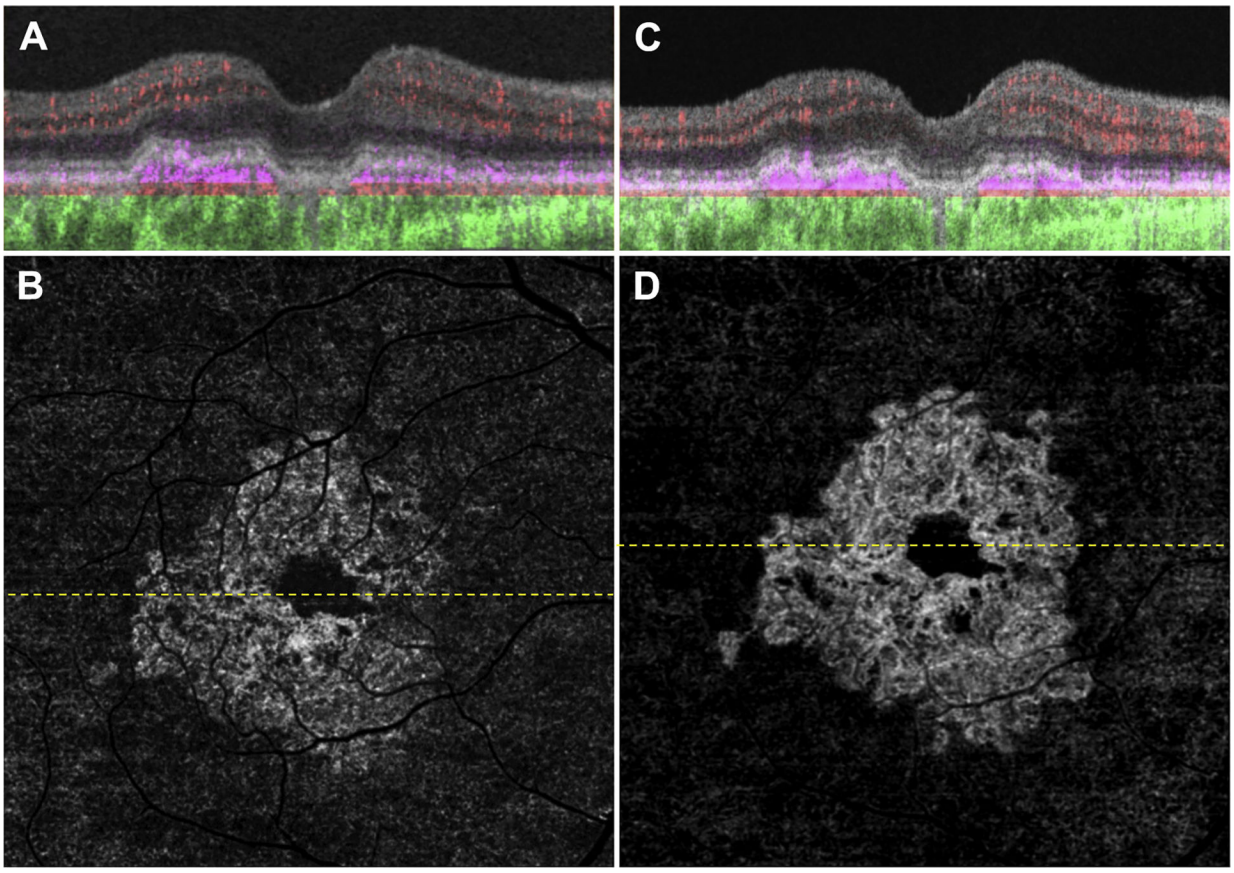

Figure 4.

Swept-source OCT angiography (OCTA) of the same eye as in Figure 3 imaged using a 6×6 mm scan. **A**, Optical coherence tomography B-scan through the fovea with color-coded flow represented as *red* for the retinal microvasculature, *pink* for the outer retina-to-choriocapillaris (ORCC) slab, and *green* for the remainder of the choroid. Note the *pink* coloration under the retinal pigment epithelium and above Bruch's membrane, which represents the type 1 macular neovascularization. **B**, Swept-source OCTA en face ORCC slab image with removal of retinal vessel projection artifacts showing a wreath-shaped neovascular complex with a total area of 7.10 mm^2.[17] The dashed line represents the B-scan contained in (**A**). The 6×6 mm scans could not be performed by the prototype SS OCTA instrument before this visit. **C**, **D**: Images obtained 14 months after those in (**A**, **B**). **C**, OCT B-scan with color-coded flow through the fovea. **D**, Swept-source OCTA en face ORCC slab image with removal of retinal vessel projection artifacts showing a neovascular lesion with an area of 7.39 mm^2. The dashed line represents the B-scan contained in (**C**).

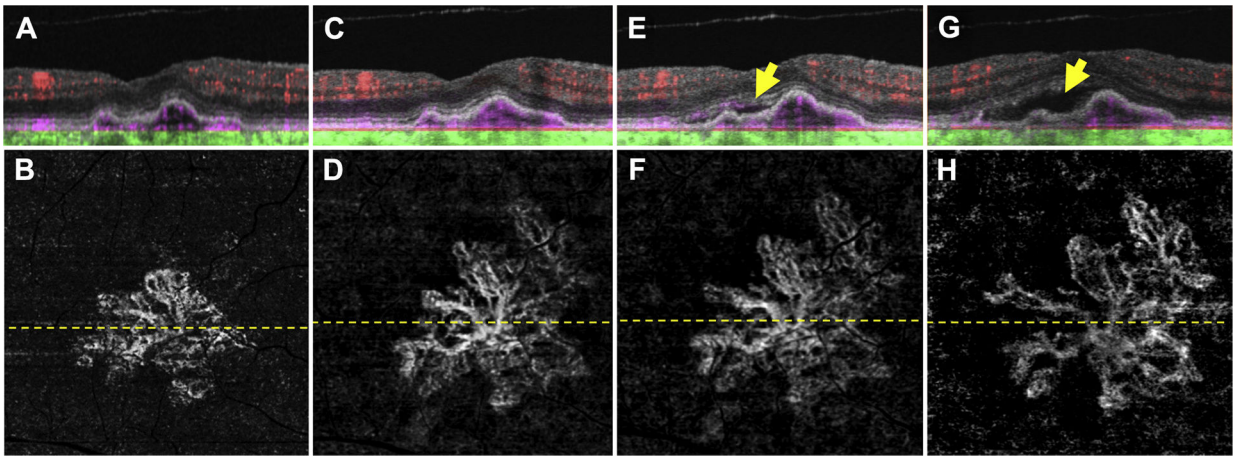

Figure 5.

Swept-source (SS) OCT angiography (OCTA; 3×3 mm) of an asymptomatic eye from a patient with nonexudative age-related macular degeneration in whom exudation developed requiring aflibercept therapy after 24 months of observation. **A**, Optical coherence tomography B-scan through the fovea with color-coded flow represented as *red* for the retinal microvasculature, *pink* for the outer retina-to-choriocapillaris (ORCC) slab, and *green* for the remainder of the choroid. Note the *pink* coloration under the retinal pigment epithelium and above Bruch's membrane, which represents the type 1 macular neovascularization. **B**, Swept source OCTA en face ORCC slab image with removal of retinal vessel projection artifacts showing a multilobular neovascular complex with a total area of 1.21 mm^2.[17] The dashed line represents the B-scan contained in (**A**). **C**, **D**: Images obtained 21 months after those in (**A**, **B**). **C**, OCT B-scan with color-coded flow through the fovea. **D**, Swept-source OCTA en face ORCC slab image with removal of retinal vessel projection artifacts showing a neovascular lesion with an area of 2.44 mm^2. The dashed line represents the B-scan contained in (**C**). **E**, **F**: Images obtained 2 months after those in (**C**, **D**). **E**, OCT B-scan with color-coded flow through the fovea showing new onset subretinal fluid (*arrow*). **F**, Swept-source OCTA en face ORCC slab image with removal of retinal vessel projection artifacts showing a neovascular lesion with an area of 2.53 mm^2. The dashed line represents the B-scan contained in (**E**). **G**, **H**: Images obtained 1 month after those in (**E**, **F**). **G**, OCT B-scan with color-coded flow through the fovea showing an increase in the amount of subretinal fluid (*arrow*). **H**, Swept-source OCTA en face ORCC slab image with removal of retinal vessel projection artifacts showing a neovascular lesion with an increase in the neovascular lesion area to 2.75 mm^2. The dashed line represents the B-scan contained in (**G**). The patient was symptomatic at this visit and intravitreal aflibercept was injected.

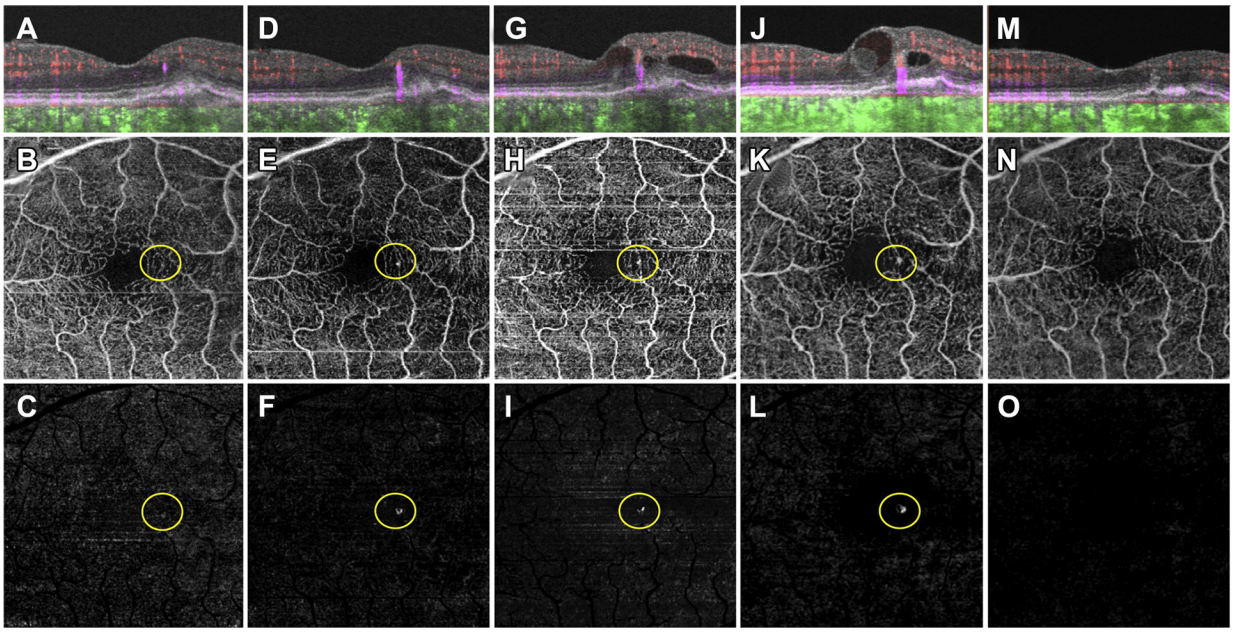

Figure 6.

Swept-source OCT angiography (OCTA; 3×3 mm) of an asymptomatic eye from a patient with nonexudative age-related macular degeneration that demonstrated exudation from type 3 macular neovascularization (MNV). **A**, Optical coherence tomography B-scan through the fovea with color-coded flow represented as *red* for the retinal microvasculature, *pink* for the outer retina-to-choriocapillaris (ORCC) slab, and *green* for the remainder of the choroid. Note the enlarging areas of *pink* coloration within the retina, which correspond to the enlarging type 3 MNV. **B**, Swept-source OCTA en face ORCC slab image showing the retinal vessel projection artifacts and a focal area of flow (*circle*) that resides within the retina. **C**, The same en face flow image shown in (**B**) after removal of the retinal vessel projection artifacts. The *circle* identifies the type 3 MNV. **D**–**F**, Images obtained 3 months after those in (**A**–**C**). **D**: OCT B-scan with color-coded flow through the fovea. Note the enlarging area of *pink* corresponding to the type 3 MNV. **E**, Swept-source OCTA en face ORCC slab image showing the retinal vessel projection artifacts and a brighter area of flow (*circle*) that resides within the retina. **F**, The same en face image shown in (**E**) after removal of retinal vessel projection artifacts. The *circle* identifies the enlarging type 3 MNV. **G**–**I**, Images obtained 1 month after the images shown in (**D**–**F**). **G**, OCT B-scan with color-coded flow through the fovea showing the type 3 MNV and intraretinal fluid. **H**, Swept-source OCTA en face ORCC slab image showing the retinal vessel projection artifacts and an area of flow (*circle*) that resides within the retina. **I**, The same image shown in (**H**) after removal of the retinal vessel projection artifacts. The *circle* identifies the type 3 MNV. **J**–**L**, Images obtained 7 months after the images shown in (**G**–**I**). **J**, OCT B-scan with color-coded flow through the fovea showing the type 3 MNV with an increase in the amount of intraretinal fluid. **K**, Swept-source OCTA en face ORCC slab image showing the retinal vessel projection artifacts and an area of flow (*circle*) that resides within the retina. **L**, The same image shown in (**K**) after removal of the retinal vessel projection artifacts. The *circle* identifies the type 3 MNV. **M**–**O**, Images obtained 10 weeks after the images shown

in (**J**–**L**) after 2 intravitreal injections of anti-vascular endothelial growth factor therapy. **M**, OCT B-scan with color-coded flow through the fovea no longer shows flow associated with the type 3 MNV. **N**, Swept-source OCTA en face ORCC slab image showing the retinal vessel projection artifacts. The area of flow previously associated with the type 3 MNV is no longer detectable. **O**, The same image shown in (**N**) after removal of the retinal vessel projection artifacts. The area of flow previous associated with the type 3 MNV is no longer detectable.

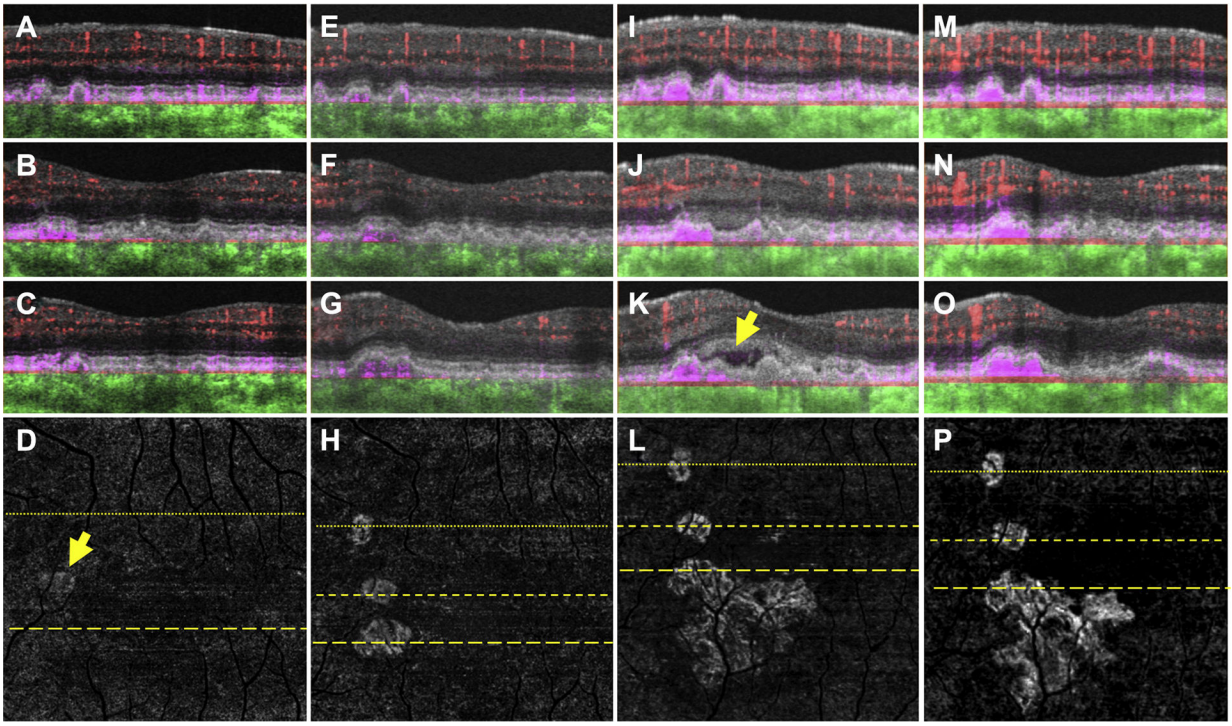

Figure 7.

Swept-source OCT angiography (OCTA; 3×3 mm) of an asymptomatic eye from a patient with nonexudative age-related macular degeneration in which exudation from 1 of 3 neovascular foci developed after 18 months of observation. (**A**–**C**) Optical coherence tomography B-scans (**A**) superior to the fovea and (**B**, **C**) through the parafoveal region with color-coded flow represented as *red* for the retinal microvasculature, *pink* for the outer retina to choriocapillaris (ORCC) slab, and *green* for the remainder of the choroid. Note the *pink* coloration under the retinal pigment epithelium and above Bruch's membrane, which represents type 1 macular neovascularization (MNV). **D**, Swept-source OCTA en face ORCC slab image with removal of retinal vessel projection artifacts showing MNV with a total area of 0.08 mm^2 (*arrow*).[17] The dotted line represents the B-scan contained (**A**), and the dashed line represents the B-scan contained in (**C**). **E**–**H**, Images obtained 13 months after those in (**A**–**D**). OCT B-scans with color-coded flow (**E**) superior to the fovea and (**F**, **G**) through the parafoveal region. **H**, Swept-source OCTA en face ORCC slab image with removal of retinal vessel projection artifacts showing the MNV with a total area of 0.30 mm^2. The dotted line represents the B-scan contained in (**E**), and the first and second dashed lines represent the B-scans contained in (**F**, **G**), respectively. **I**–**L**, Images obtained 5 months after those in (**E**–**H)**. OCT B-scans with color-coded flow (**I**) superior to the fovea and (**J**, **K**) through the parafoveal region. Only 1 of the neovascular foci appears to be associated with new onset exudation (**K**, *arrow*). **L**, Swept-source OCTA en face ORCC slab image with removal of retinal vessel projection artifacts showing the MNV with a total area of 1.24 mm^2. The dotted line represents the B-scan contained in (**I**), and the first and second dashed lines represent the B-scans contained in (**J**, **K**), respectively. **M**–**P**, Images obtained 2 months after those in (**I**–**L**) after 2 intravitreal injections of anti-vascular endothelial growth factor (VEGF) therapy. OCT B-scans with color-coded flow (**M**) superior to the fovea and

(**N**, **O**) through the parafoveal region. The exudation seen previously has resolved. **P**, Swept-source OCTA en face ORCC slab image with removal of retinal vessel projection artifacts showing the MNV with a total area of 1.21 mm^2. The dotted line represents the B-scan contained in (**M**), and the first and second dashed lines represent the B-scans contained in (**N**, **O**), respectively. After anti-VEGF therapy, no significant change in the configuration of the MNV can be appreciated.

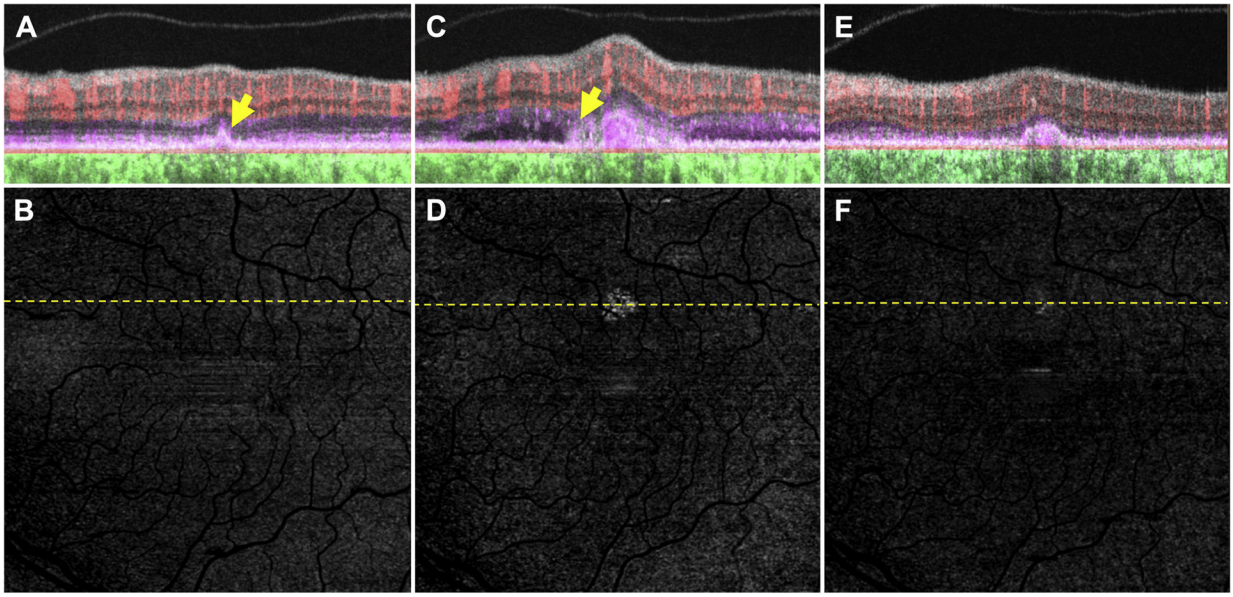

Figure 8.

Swept-source OCT angiography (OCTA; 3×3 mm) of an asymptomatic eye from a patient with nonexudative age-related macular degeneration without evidence of subclinical macular neovascularization (MNV) in which exudation developed associated with subretinal hyperreflective material (SHRM). **A**, Optical coherence tomography B-scan superior to the fovea with color-coded flow represented as red for the retinal microvasculature, *pink* for the outer retina to choriocapillaris (ORCC) slab, and *green* for the remainder of the choroid. The *arrow* corresponds to a druse that was not associated with a flow signal. **B**, Swept-source OCTA en face ORCC slab image with removal of retinal vessel projection artifacts. No obvious flow signal can be identified. The dashed line represents the B-scan contained in (**A**). **C**, **D**: Images obtained 2 months after those in (**A**, **B**). **C**, OCT B-scan with color-coded flow superior to the fovea shows a neovascular lesion that is associated with subretinal fluid and SHRM (*arrow*). **D**, Swept-source OCTA en face ORCC slab image with removal of retinal vessel projection artifacts showing evidence of the MNV. The dashed line represents the B-scan contained in (**C**). **E**, **F**: Images obtained 3 months after those in (**C**, **D**) after 3 intravitreal injections of anti-vascular endothelial growth factor (VEGF) therapy. **E**, OCT B-scan with color-coded flow superior to the fovea. The neovascular lesion resides under the retinal pigment epithelium and persists as a type 1 neovascular lesion. **F**, Swept-source OCTA en face ORCC slab image with removal of retinal vessel projection artifacts showing the MNV that appears smaller after anti-VEGF therapy. The dashed line represents the B-scan contained in (**E**).

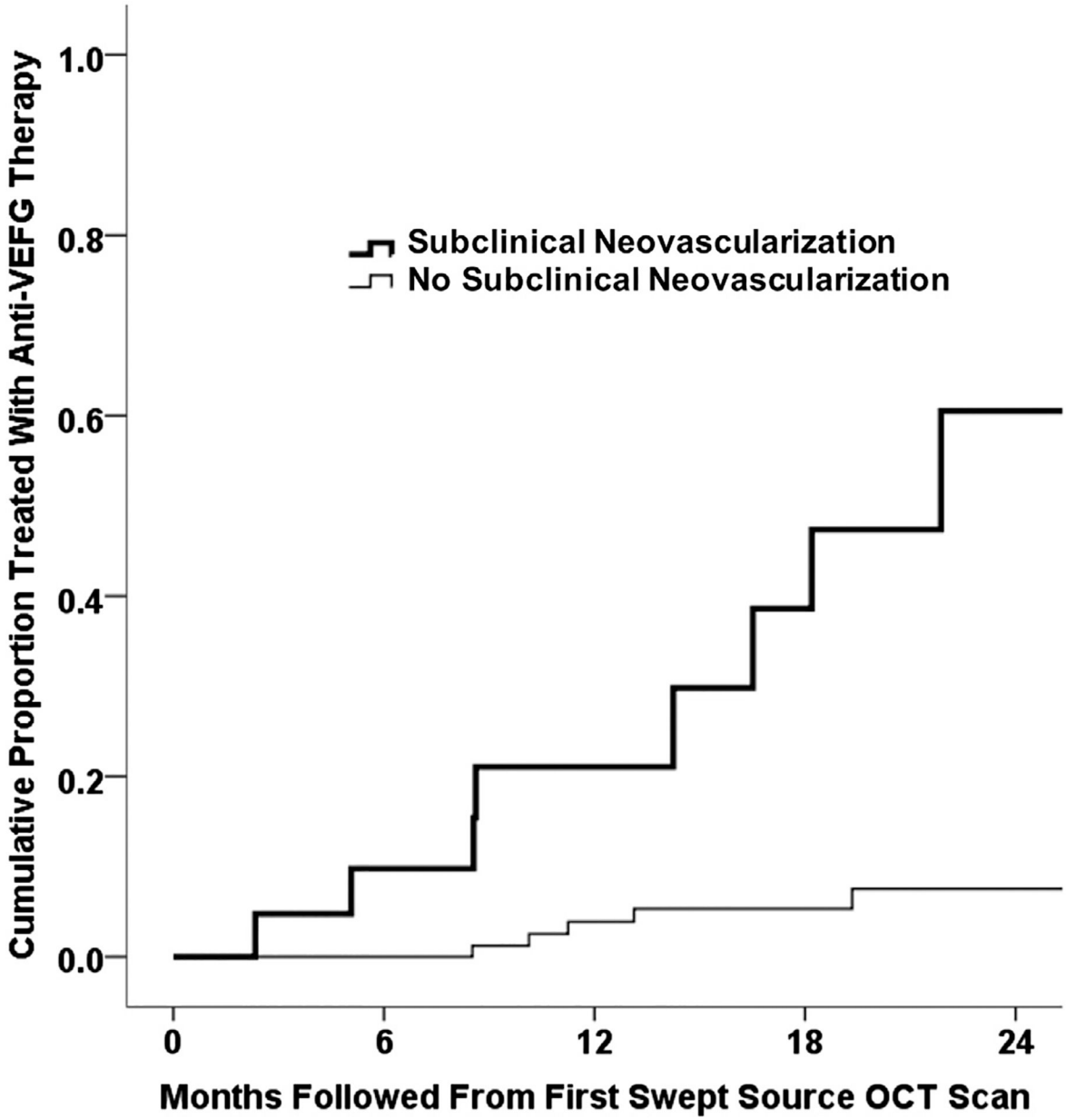

Figure 9.

Kaplan-Meier analysis showing the cumulative proportion of eyes treated with anti–vascular endothelial growth factor (VEGF) therapy from the time of the first swept-source (SS) OCT angiography (OCTA) scan. For eyes with subclinical macular neovascularization (MNV) at the time of first SS OCTA imaging, the incidence of exudation after 12 months was 21.1%. For eyes without subclinical MNV at the time of first SS OCTA imaging, the incidence of exudation after 12 months was 3.6%.

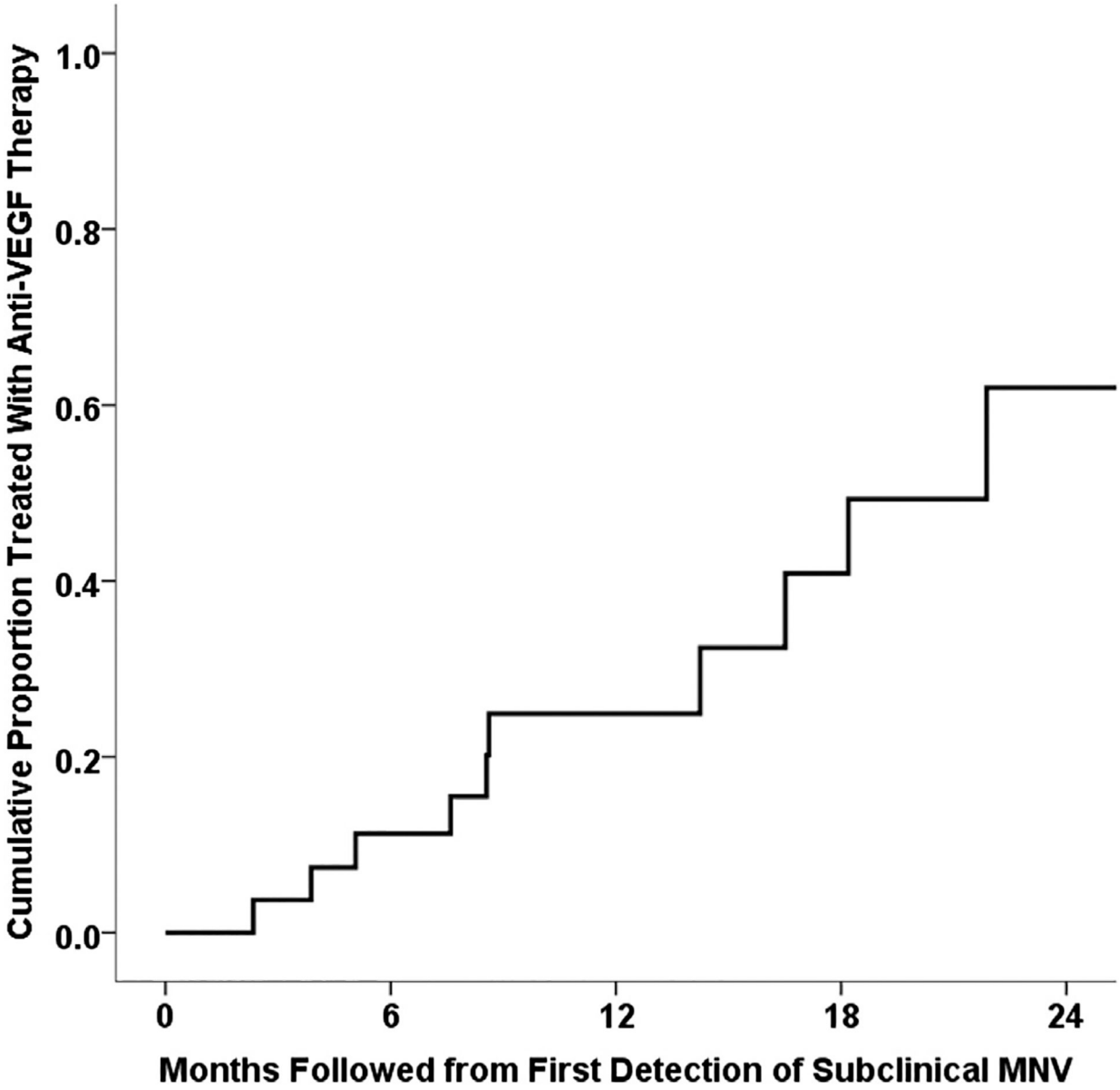

Figure 10.

Kaplan-Meier analysis of the cumulative proportion of eyes treated with anti–vascular endothelial growth factor (VEGF) therapy from the time of first detection of subclinical macular neovascularization (MNV). The overall incidence of exudation from detection of any subclinical MNV was 24% at 1 year of follow-up.